

Investigation of cavitation in real size diesel injection nozzles

C. Badock^a, R. Wirth^{a,*}, A. Fath^b, A. Leipertz^b

^a Robert Bosch GmbH, FV/SLE3-Sh, Postfach 10 60 50, D-70049 Stuttgart, Germany

^b Universität Erlangen-Nürnberg, LTT, Am Weichselgarten 8, D-91058 Erlangen, Germany

Abstract

The laser light sheet and shadowgraph techniques have been applied to investigate cavitation phenomena in the spray hole of real size diesel injection nozzles and the breakup at the spray hole exit. The experiments were performed with a Bosch Common Rail system for generating unsteady injection conditions. Rail pressures up to 60 MPa were used. The diesel-like test oil was injected into a chamber which could be pressurized up to 1.5 MPa. The local position and range of cavitation films, lying between the flow and the nozzle wall, as well as single cavitation bubbles could be observed at different times of the injection process. The pictures of the light sheet experiment taken with a CCD camera were compared with photographs taken by the shadowgraph technique under the same injection conditions. As a result the cavitation films could be observed as thin objects which do not extend into the internal flow of the injection nozzle. In addition, even under higher injection pressures, no accumulation or foam of bubbles could be noticed in the spray hole. This leads to the conclusion that there is an intact liquid core leaving the nozzle even at high injection pressures. Further experiments dealt with the coherence of flow conditions at the start of injection and the spray patterns produced at the beginning of the injection process. These measurements were made with a special optical setup including a high-speed ICCD camera. © 1999 Elsevier Science Inc. All rights reserved.

1. Introduction

In order to understand the whole breakup process of a diesel spray, it is necessary to determine the phenomena which lead to primary and secondary breakup caused by interaction with the dense gas phase and collision with other liquid elements. The knowledge of the spray forming phenomena is essential to allow predictions of the spray behaviour and the mixture preparation during the injection process. To reach future emission standards, the fuel distribution inside the combustion chamber and the droplet size distribution must be controlled appropriately.

The present paper describes the properties of the internal flow of a diesel injection nozzle and in particular the cavitation which is often considered to be the main reason for primary breakup (Chaves et al., 1995; Hiroyasu et al., 1991; Reitz and Bracco, 1982; Roosen et al., 1997; Soteriou et al., 1995; Tamaki et al., 1997). By changing the flow field inside the nozzle through the internal design, e.g. size and arrangement of the holes or the hydro-grinding of the inlet edge, the spray behaviour can be strongly influenced (Kampmann et al., 1996). However, in most cases the characteristics of the flow field in a single nozzle hole are unknown and not accessible for measurements. Even with transparent nozzles in original size, with spray hole diameters less than 300 µm, the optical access by the

shadowgraph technique is difficult because of the total reflection by cavitation films lying around the liquid (Badock et al., 1997; Chaves et al., 1995).

The injection pressures resulting in cavitation phenomena are relatively low so that, even in case of unsteady pressure conditions, for nearly all the duration of the injection process the spray hole is surrounded by cavitation films (Eifler, 1990). The laser light sheet technique has often been used to characterize the spray breakup (Cavaliere et al., 1988; Fath et al., 1996, 1997; Gülder et al., 1992; Nishida et al., 1992; Smallwood et al., 1994) and to investigate the existence of a liquid core in the near nozzle region (Cavaliere et al., 1988; Fath et al., 1996, 1997; Gülder et al., 1992; Smallwood et al., 1994). The advantage of this technique is the high resolution with a very thin light sheet so that its application also seems promising to determine the structure of the cavitation films by using a real size nozzle with cylindrical hole shape. The results are compared with shadowgraph measurements to determine the cavitation film length. Further, light sheet measurements analyse the atomizing jet in the near nozzle region with respect to observations of the spreading of an intact liquid core. Other techniques using two-dimensional nozzles (Dan et al., 1997; Hiroyasu et al., 1991; Kent and Brown, 1983; Senda et al., 1997) do not represent correctly geometric influences such as exact flow through needle seat and sac hole and, besides this, the behaviour of the cavitation may be different.

Observation of the spray structure at the start of injection shows different shapes (Eifler, 1990; Takahashi et al., 1997) and the use of a high-speed camera helps to correlate the state of the flow with mushroom-like spray shapes and pre-jets that are observed.

* Corresponding author. E-mail: ralf.wirth@de.bosch.com

2. Experimental setup

For investigating the internal flow under diesel injection-like conditions a standard type nozzle is used. The nozzle tip is replaced by perspex modelling a sac and spray hole (Fig. 1). The hole diameter d can be varied between $d=0.18$ mm and $d=0.30$ mm by changing the nozzle tip whereas the length l of the hole is kept constant so a l/d ratio between 3.3 and 5.6 can be achieved. The complete experimental setup is shown in Fig. 2.

A Bosch Common Rail system is used to provide unsteady injection conditions. The main advantage of this system is the free choice of injection time and pressure which is independent of engine speed.

High rail pressures decrease the lifetime of the perspex nozzle tip because the perspex is weakened by the strong pressure wave at the start of injection. During the measurements it is difficult to detect possible damage. Most of the measurements are performed at low rail pressures of, e.g., $p_R = 25$ MPa, where the acrylic is very rigid. With the maximum rail pressure of $p_R = 60$ MPa too few (≈ 20) injections have been investigated to be sure that the geometry, especially the inlet edge of the spray hole, is not damaged during the experiment.

The fluid used is a test oil with diesel-like physical properties. In particular, the values of density, viscosity and surface tension are the same as for diesel fuel. Another advantage of the test oil is a good correspondence in the refractive index n to that of perspex ($n_{oil} = 1.46$, $n_{perspex} = 1.49$). So, total reflection and refraction will only occur at the outer surface of the cylinder.

As a light source a frequency-doubled Nd:YAG-laser ($\lambda = 532$ nm) is used. With a pulse duration of 10 ns, a short exposure time is achieved which is needed because of the high flow velocities of about 200 m/s. An optical setup produces a calculated light sheet thickness of less than 20 μm (Fig. 3). It is possible to vary the position of the light sheet inside the nozzle or the free jet (Fig. 4). With micro-screws a precise adjustment is achieved and the small focal depth of the detection optics is helpful for the manual positioning.

The internal flow and the free jet have different focal planes. It turned out that by adjusting the light sheet to the internal flow, the scattering light of the free jet disturbed the desired signal and vice versa.

Perpendicular to the spray axis and the light sheet, an optical system consisting of a long-distance-microscope and a

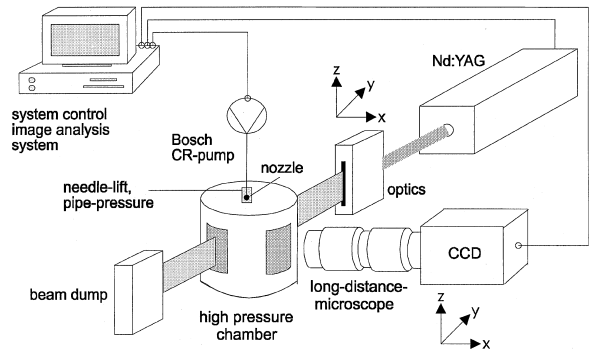


Fig. 2. Experimental setup for light sheet measurements.

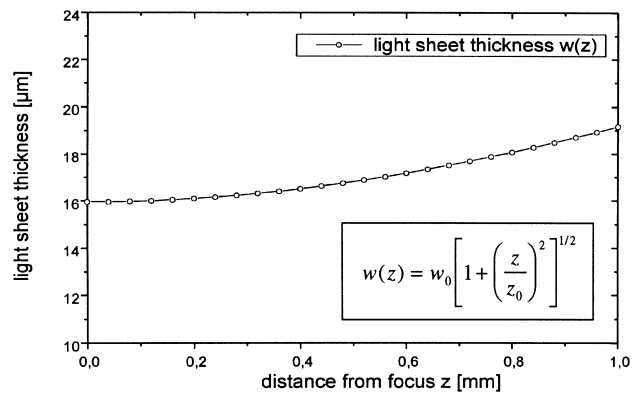


Fig. 3. Calculated light sheet thickness.

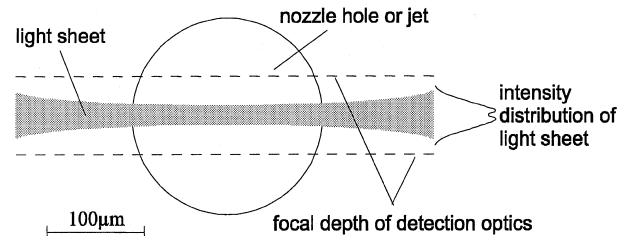


Fig. 4. Possible position of the laser light sheet in the nozzle or the free jet.

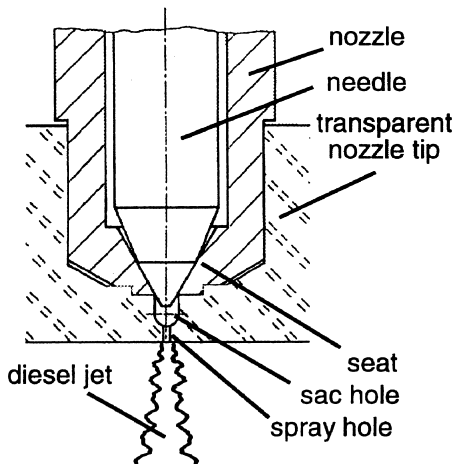


Fig. 1. Transparent diesel nozzle.

CCD camera, is built up. With the high optical resolution it is possible to project the spray hole on the full CCD-chip. The camera can be triggered externally so that the moment of exposure is adjustable with any desired delay with respect to the start of injection. The images are transferred digitally to an image-analysing and postprocessing computer.

To realize high gas densities the liquid is injected into a pressure chamber with optical access. The applied back pressures range between $p_c = 0.1$ and 1.5 MPa.

For the high-speed imaging a different optical setup is used (Fig. 5). The Hadland Photonics IMACON 468 camera has eight channels, each fitted with a CCD and a gated MCP intensifier. The framing speed is only limited to the minimum exposure time of 10 ns. As light source a Xenon-flash with a pulse energy of 375 J is used. The investigations focus on the unsteadiness of internal flow and the breakup process at the start of injection.

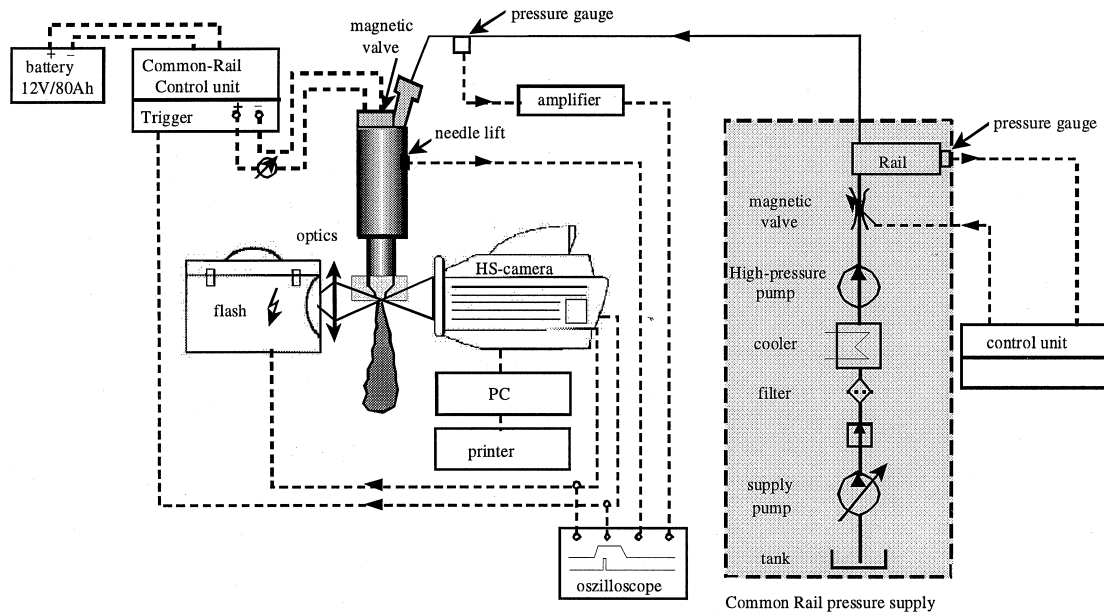


Fig. 5. Experimental setup for high-speed photography.

3. Investigations under unsteady injection pressures

For interpreting the recorded images all mechanisms that may lead to the observed images have to be considered. As shown in Fig. 6, multiple reflection and secondary refraction of the laser light sheet cause signals which can lead to misinterpretations. The different scattering phenomena in the internal flow and the free jet have to be taken into consideration. The most important difference is the fact that inside the nozzle the phase boundary between the perspex and the cavitation is limited by the surface roughness of the drilled holes. The free jet is characterized by primary and secondary breakup mechanisms so that there is a rough and stochastic surface with unpredictable scattering properties. As will be shown later the multiple scattering will cause a milky haze lying in front of the observed plane. In the near-nozzle region and for the case of no secondary breakup, the disturbing effects are reduced to a minimum and a measurement of the size of the intact liquid core is possible. The very thin light sheet and the correctly adjusted laser intensity reduces the amount of the disturbing scattered light.

Similar problems will occur while observing the internal flow. If the surface between the cavitation films and the fluid is rough, additional reflection and refraction is likely. Further, the existence of many small phase boundaries resulting for example from a cluster of cavitation bubbles as referenced in Soteriou et al. (1995) should lead to a hazy plane as in the free jet. Problems with interpreting the results achieved with the laser light sheet technique have already been discussed in Cavaliere et al. (1988), Gülder et al. (1992) and Smallwood et al. (1994). Another difficulty arises from coupling the light sheet into the perspex: the optical path-length in comparison to air is increased because of the higher refractive index. So, the tail of the light sheet has to be newly positioned horizontally when the object plane is switched between the inside and outside of the nozzle.

The flow velocity through the nozzle is mainly affected by the feed pressure and the needle lift. By changing the rail pressure, the dynamic of the needle opening and closing is also different (Fig. 7). It can be shown that the applied back pressures do not influence the needle dynamics. The maximum needle lift for the Common Rail injector used is $h_{\max} = 0.2$ mm.

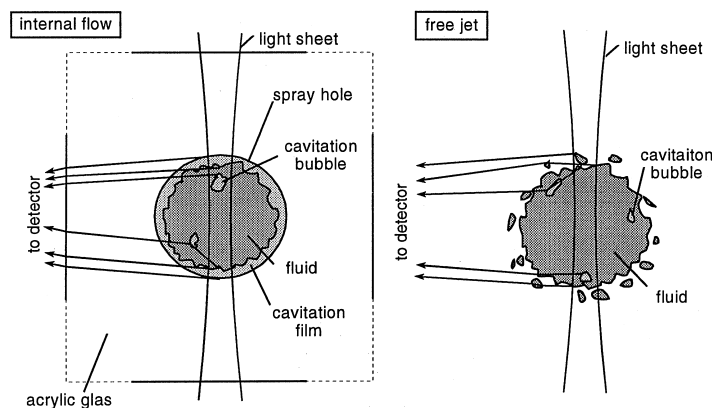


Fig. 6. Interaction between light sheet and phase boundaries.

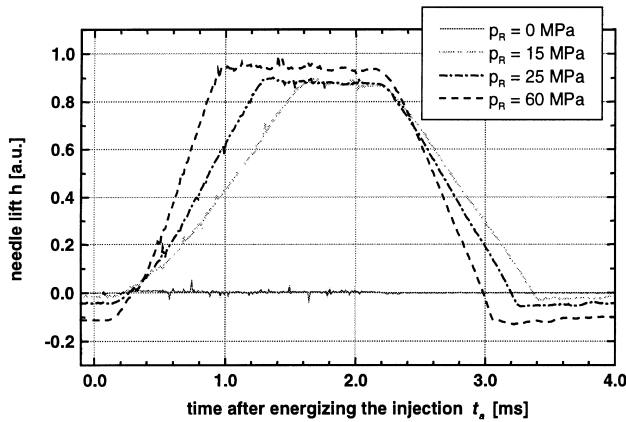


Fig. 7. Needle lift for different rail pressures.

The needle spring force is reduced so that the injector opens even at rail pressures below 15 MPa.

Fig. 8 shows a sequence of the internal flow in the spray hole at different times t_a after energizing the injector. The spray hole is marked by two lines – the beginning of the line represents the inlet edge, the end of the line shows the nozzle exit. The strongest scattering signal is detected on the right side of the spray hole facing the laser light sheet (Fig. 2). The rail pressure is kept constant at $p_R = 25$ MPa whereas the chamber pressure is at its maximum value of $p_c = 1.5$ MPa. In this case a spray hole with a diameter of $d = 0.20$ mm is used.

For comparison, in Fig. 9 the corresponding images taken by the shadowgraph technique are presented. In contrast to Fig. 8 the complete transparent geometry is shown. It should be mentioned that the images are not taken from a single injection but every picture is a detail of another injection. Small cycle-to-cycle fluctuations may result in deviations in the length of the cavitation films especially at the start or at the end of injection. So, for every parameter setting, a sequence of about 20 pictures is recorded and the representative ones are shown.

At the beginning of the injection large gas bubbles can be observed in the sac hole. These bubbles may remain in the orifice during the time between the injections so that they are

probably filled with air. Additional air is sucked into the spray hole during the first stages of the needle opening. Afterwards these large air bubbles are flushed out of the nozzle with the liquid. This occurs at $t_a = 300$ μ s after start of energizing the injector. Figs. 8 and 9 show different pictures of the same phenomena. The smooth phase boundary between the air bubble and the nozzle wall should also result in a very thin scattering signal depending on the light sheet thickness. So the first picture of the sequence demonstrates the resolution of this technique. Between $t_a = 380$ μ s and $t_a = 400$ μ s the growth of the cavitation films can be observed. Within 20 μ s the cavitation extends nearly through the entire spray hole.

Even in the case when the cavitation films reach the nozzle exit a continuous liquid core surrounded by cavitation is visible. In the shadow images sometimes bright points are recognized. This indicates the irregularity and the very small thickness of the cavitation film. At the point with the highest flow velocity (quasi-steady case: $t_a = 2200$ μ s) the films appear more regular as shown in Fig. 8. A single cavitation bubble with an elliptical shape is observed in the lower part of the spray hole. It is clear that such phenomena cannot be detected by the shadowgraph techniques. The closing process of the needle produces similar images as in the opening phase. The different appearance of the internal flow at the start and at the end of injection ($t_a > 3200$ μ s) may be a result of small geometry defects that differ between the two test objects. Deviations in cavitation inception influenced by the quality of the inlet corner are discussed for example in Arai et al. (1988), Hiroyasu et al. (1991), Kent and Brown (1983) and Tamaki et al. (1997).

The influence of rail pressure and chamber pressure on the cavitation is shown in Fig. 10. Transparent nozzle tips with spray hole diameter $d = 0.20$ mm and hole length $l = 1.0$ mm are used in this experiment. To compare the internal flow at different pressure conditions any effects from the needle dynamics have to be excluded. Therefore $t_a = 2200$ μ s (maximum needle lift and quasi-steady flow conditions) is chosen. In part A of Fig. 10 the chamber pressure is 1.5 MPa and the rail pressure is varied between $p_R = 15$ MPa and $p_R = 60$ MPa. The difference in the pictures may be caused by cycle to cycle fluctuations. The chamber pressure variation (part B of Fig. 10) explored at a rail pressure of $p_R = 25$ MPa shows nearly the same result. The limited quality of the images can only allow the conclusion that, for all pressure conditions, the cavitation films have quite similar dimensions. Nevertheless, an increased

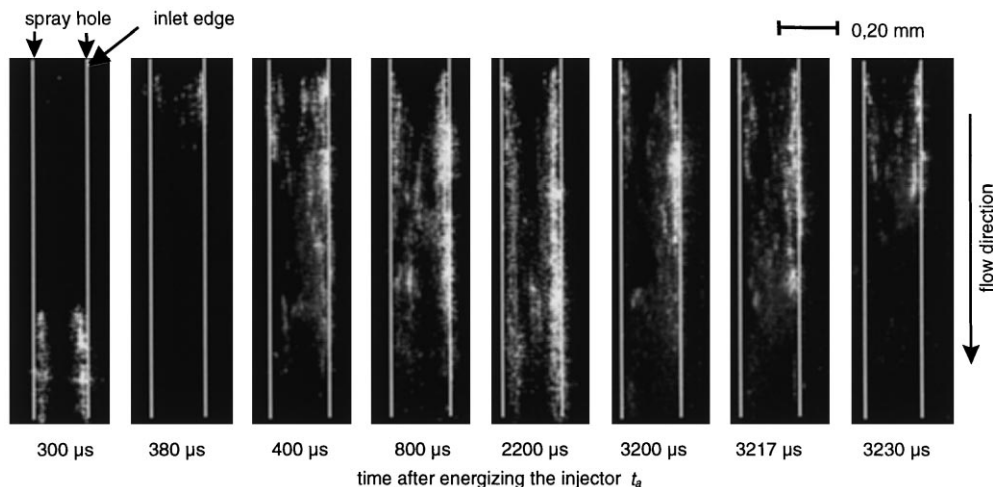


Fig. 8. Scattering signal of the internal flow: $p_R = 25$ MPa, $p_c = 1.5$ MPa, energizing time $t_e = 2$ ms, spray hole diameter $d = 0.20$ mm, length $l = 1.0$ mm.

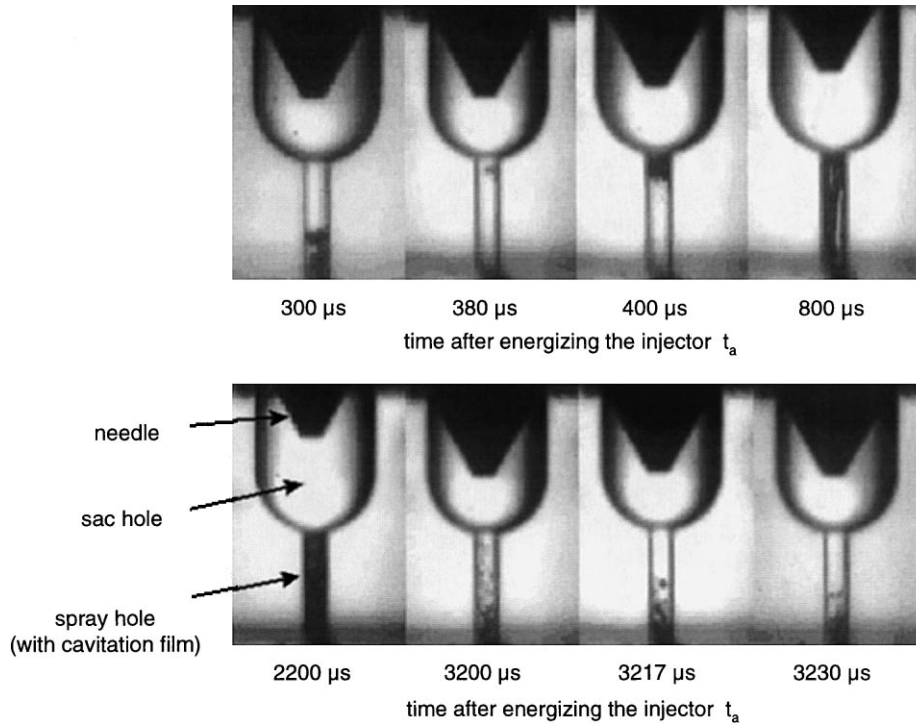


Fig. 9. Cavitation inside the spray hole under unsteady pressure conditions: $p_R = 25$ MPa, $p_c = 1.5$ MPa, energizing time $t_e = 2$ ms, spray hole diameter $d = 0.20$ mm, length $l = 1.0$ mm.

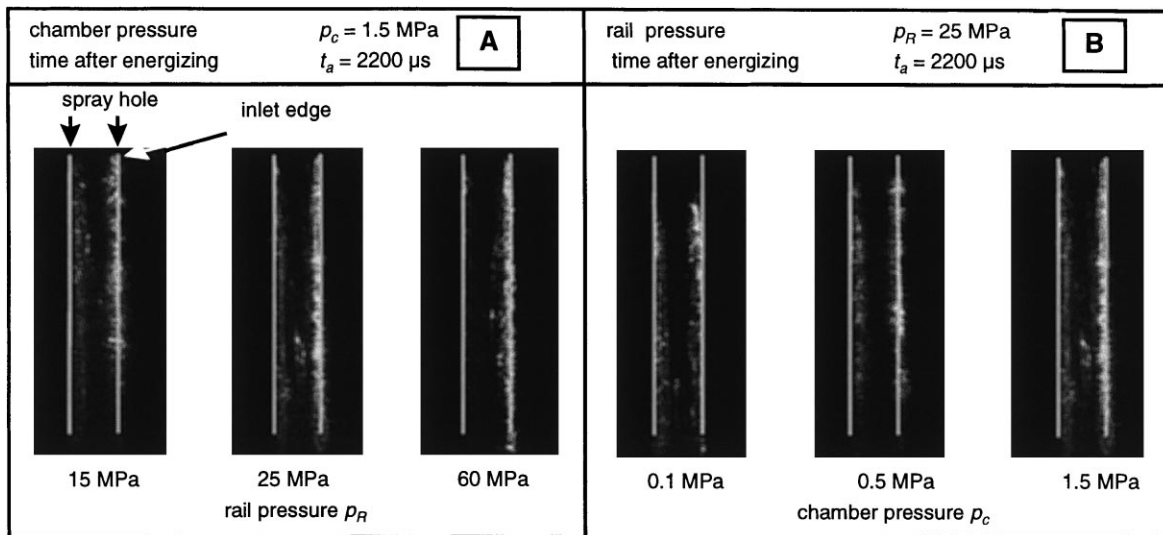


Fig. 10. Cavitation films in the internal flow under variation of rail pressure and chamber pressure.

interaction of cavitation and turbulence in the flow can be assumed that will result in unsteady effects in the behaviour of the cavitation films (Kampmann et al., 1996).

A large intact liquid core inside the flow is visible at all pressure conditions. Sometimes single cavitation bubbles or disruptions from cavitation films can be observed. No foam or any accumulation of many small bubbles is noticed – such phenomena would produce a milky scattering signal which is not detected.

The laser light sheet technique was also applied to investigate the spray structure outside the nozzle. Such measurements

have already been presented and discussed in Fath et al. (1996, 1997). With the knowledge about the intact liquid core at the nozzle exit it is interesting to compare internal flow and spray structure. The scattering images (Fig. 11) are shown together with shadowgraphs (Fig. 12). This is useful in the case of few scattering signals to get an impression about the shape of the spray. The ligaments at the end of injection are characteristic of this.

The mushroom-like structure at the start of injection is stochastic and cannot be compared directly between the two image series. Also, the absolute start of injection fluctuates by ± 10 μ s.

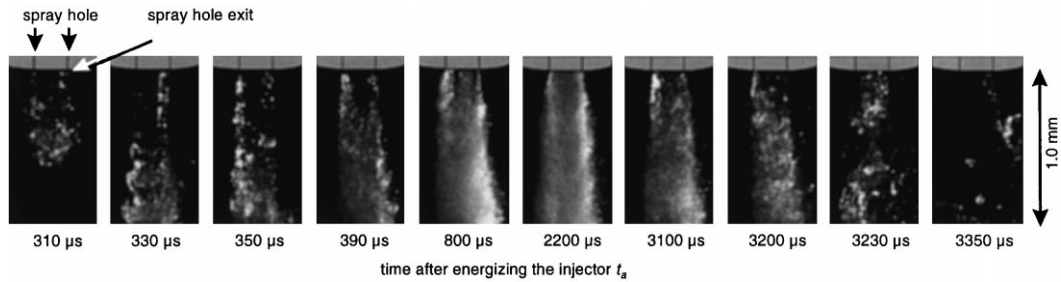


Fig. 11. Free jet in the near nozzle region with the laser light sheet technique: $p_R = 25$ MPa, $p_c = 1.5$ MPa, energizing time $t_c = 2$ ms, spray hole diameter $d = 0.20$ mm, length $l = 1.0$ mm.

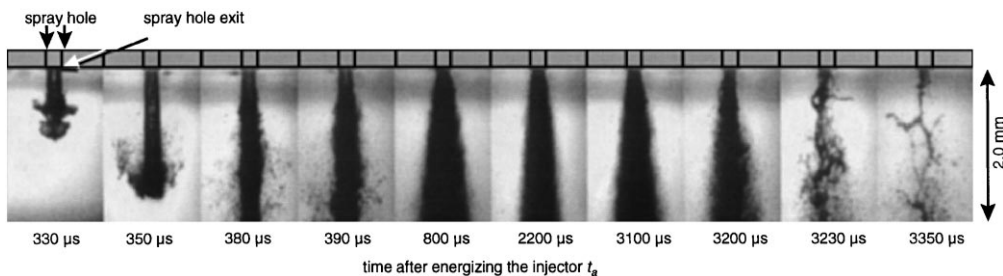


Fig. 12. Free jet in the near nozzle region with the shadowgraph technique: $p_R = 25$ MPa, $p_c = 1.5$ MPa, energizing time $t_c = 2$ ms, spray hole diameter $d = 0.20$ mm, length $l = 1.0$ mm.

The light sheet images show an intact liquid core. This fact cannot be proved by the shadowgraph images. From $t_a = 330$ – 390 μ s only a smooth surface of the free jet can be observed (Fig. 12). During the needle opening the flow velocity inside the spray hole increases and the zone of primary and secondary breakup moves towards the nozzle exit. It was previously mentioned that the surface of atomized ligaments and droplets causes a hazy effect which makes the optical access to the internal structures difficult – so an existing intact liquid core, which does not give any optical signal, is not visible. Just by interpreting the light sheet sequence (Fig. 11) it seems that the intact liquid core disappears at high flow velocities ($t_a > 800$ μ s). But the results from the observations of the internal flow make this hypothesis improbable.

4. Spray structures at the start of injection

During the needle closing dissolved gas occurs in the sac hole and the spray hole in the form of large bubbles. The fact that the bubbles survive the time between two injections leads to the conclusion that they possess only a very small part of vapour.

At the start of injection the bubbles in the spray hole are partly sucked into the sac hole. If the nozzle leaves the seat throttling, a pressure wave strongly compresses the bubbles which can be seen in Fig. 13. The compressed bubbles and the liquid are pushed out together. Outside the nozzle the gas bubble expands because of the lower ambient pressure. In upstream direction the liquid column is influenced by the expansion forces which leads to the mushroom-like shape (Fig. 14A). Also, the interaction of the jet tip with the gas phase will amplify to build such phenomena by stripping the boundary layers off the jet surface and pushing them aside.

If the bubble lies in front of the jet a thin pre-jet is ejected in the direction of the spray (Fig. 14B). The energy of this pre-jet might be high enough to move during a time of at least 30 μ s with the same speed of the following liquid. Afterwards the acceleration of the nozzle flow will help to overtake the pre-jet, which is not shown here. The pre-jet does not show breakup phenomena in most cases. Only at the tip of the jet can the same mushroom-like structure as at the main jet be observed. This leads to the assumption that the pre-jet contains only laminar flow. The influence on the mixture preparation can be neglected because of the short life time and the lack of breakup.

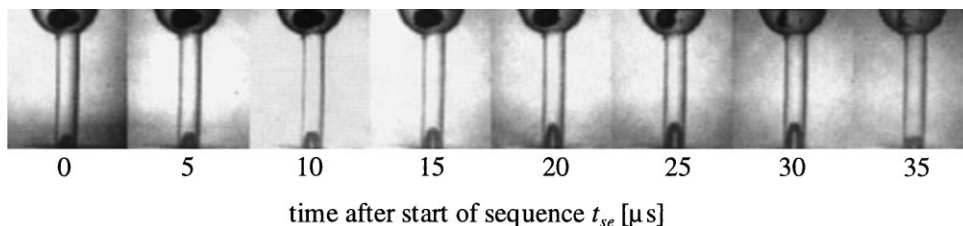


Fig. 13. Internal flow at start of injection with the shadowgraph technique, $p_R = 25$ MPa, $p_c = 1.5$ MPa, energizing time $t_c = 2$ ms, spray hole diameter $d = 0.20$ mm, length $l = 1.0$ mm.

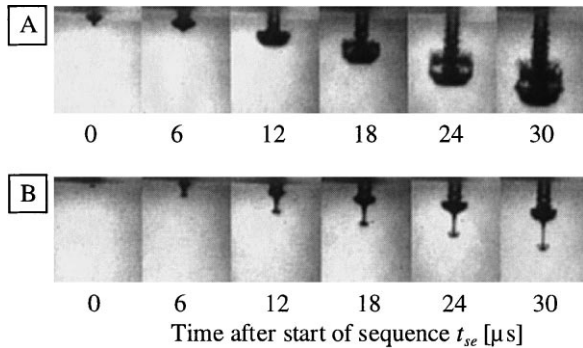


Fig. 14. Free jet in the near nozzle region at start of injection with shadowgraph technique: $p_R = 25$ MPa, $p_c = 1.5$ MPa, energizing time $t_c = 2$ ms, spray hole diameter $d = 0.20$ mm, length $l = 1.0$ mm.

5. Conclusions

The laser light sheet technique has been applied to investigate the internal flow of cavitated real size diesel injection nozzles. In comparison with images taken by the shadowgraph technique it is shown that the scattering signal leads to the same length of cavitation films inside the spray hole. Furthermore, the light sheet technique enables a view of the core of the flow which is covered by cavitation films and not visible with shadowgraph. Single cavitation bubbles or disturbances from the cavitation films can be detected and the existence of a cavitation foam or many small bubbles inside the nozzle holes can be discounted. Even at fuel pressures up to 60 MPa the hole is filled with liquid surrounded by cavitation films.

The scattering images are too blurred to be useful for quantitative measurements of the cavitation film thickness. The determination of this parameter is necessary to compare experimental data with calculated results of cavitation models. Nevertheless, the laser light sheet technique is promising for further progress in this field.

The results from the internal flow lead to the hypothesis that, under diesel-like pressure conditions, an intact liquid core leaves the nozzle holes.

High-speed photography helps to understand the occurrence of the pre-jet during the first stage of the injection. A correlation between gas bubbles in the nozzle hole and the observation of the pre-jet can be found. A significant influence of this phenomenon on the mixture preparation is not expected.

References

Arai, M., Shimizu, M., Hiroyasu, H., 1988. Breakup length and spray formation mechanism of a high speed liquid jet. In: Proceedings of ICLASS-88, pp. 177–184.

Badock, C., Wirth, R., Kampmann, S., Tropea, C., 1997. Fundamental study of the influence of cavitation on the internal flow and atomization of diesel sprays. In: Proceedings of ILASS-97, Florence, Italy, pp. 53–59.

Cavaliere, A., Ragucci, R., D'Alessio, A., Noviello, C., 1988. Analysis of diesel sprays through two-dimensional laser light scattering. In: Proceedings of 22nd Symposium on Combustion 1988, Seattle, USA, pp. 1973–1981.

Chaves, H., Knapp, M., Kubitzek, A., Obermeier, F., Schneider, T., 1995. Experimental Study of Cavitation in the Nozzle Hole of Diesel Injectors Using Transparent Nozzles, SAE 950290.

Dan, T., Yamamoto, T., Senda, J., Fujimoto, H., 1997. Effect of nozzle configurations for characteristics of non-reacting diesel fuel spray. In: Proceedings of ICLASS-97, Seoul, Korea, pp. 259–274.

Eifler, W., 1990. Untersuchungen zur Struktur des instationären Dieselloleinspritzstrahles im Düsenbereich mit der Methode der Hochfrequenzkinematographie. Ph.D Thesis, University of Kaiserslautern.

Fath, A., Münch, K.-U., Leipertz, A., 1996. Spray breakup of diesel fuel close to the nozzle. In: Proceedings of ILASS-96, Lund, Sweden, pp. 59–64.

Fath, A., Münch, K.-U., Leipertz, A., 1997. Spray breakup process of diesel fuel-investigated close to the nozzle. In: Proceedings of ICLASS-97, Seoul, South Korea, pp. 513–519.

Gülde, Ö.L., Smallwood, G.J., Snelling, D.R., 1992. Diesel Spray Structure Investigation by Laser Diffraction and Sheet Illumination, SAE 920577.

Hiroyasu, H., Arai, M., Shimizu, M., 1991. Breakup length of a liquid jet and internal flow in a nozzle. In: Proceedings of ICLASS-91, Gaithersburg, USA.

Kampmann, S., Dittus, B., Mattes, P., Kirner, M., 1996. The Influence of Hydro Grinding at VCO Nozzles on the Mixture Preparation in a DI Diesel Engine, SAE 960867.

Kent, J.C., Brown, G.M., 1983. Nozzle exit flow characteristics for square-edged and rounded inlet geometries. Combustion Science and Technology 30, 121–132.

Nishida, M., Nakahira, T., Komori, M., Tsujimura, K., Yamaguchi, I., 1992. Observation of High Pressure Fuel Spray with Laser Light Sheet Method, SAE 920459.

Reitz, R.D., Bracco, F.V., 1982. Mechanism of atomization of a liquid jet. Phys. Fluids 25 (10), 1730–1742.

Roosen, P., Unruh, O., Behmann, M., 1997. Investigation of cavitation phenomena inside fuel nozzles. In: Proceedings of ISATA-97.

Senda, J., Dan, T., Yamamoto, T., Fujimoto, H., 1997. Fuel flow characteristics and cavitation phenomena in nozzle of diesel spray by planer acrylic model. In: Proceedings of ICLASS-97, Seoul, Korea, pp. 215–222.

Smallwood, G.J., Gülde, Ö.L., Snelling, D.R., 1994. Tomographic visualization of the dense core region in transient diesel sprays. In: Proceedings of ICLASS-94, Rouen, France, pp. 270–277.

Soteriou, C., Andrews, R., Smith, M., 1995. Direct Injection Diesel Sprays and the Effect of Cavitation and Hydraulic Flip on Atomization, SAE 950080.

Takahashi, H., Kono, M., Yanagisawa, H., Shiga, S., Karasawa, T., Nakamura, H., 1997. Initial atomization of an intermittent spray from a diesel nozzle. In: Proceedings of ICLASS-97, Seoul, South Korea, pp. 529–536.

Tamaki, N., Nishida, K., Hiroyasu, H., Shimizu, M., 1997. Effects of the internal flow in a nozzle hole on the breakup processes of a liquid jet. In: Proceedings of ICLASS-97, Seoul, South Korea, pp. 417–424.